Power-Independent Microwave Instantaneous Frequency Measurement Based on Combination of Brillouin Gain and Loss Spectra

Xin Wang, Yong-Lan Yang, Yu-Qiu Xu, Yue Cao, and Wei-Wen Zou, *Senior Member, IEEE*

***Abstract*—Photonics-assisted microwave instantaneous frequency measurement (IFM) is considered as a promising technique for detecting an unknown radio-frequency (RF) signal, which has advantages of broad frequency measurement range and fast processing speed. Up to date, there is no photonics-assisted IFM system that can essentially measure an unknown RF signal time-frequency information with power fluctuating seriously. Moreover, the measurement accuracy and frequency modulation recognition are not as good as those of traditional electronic methods. Here, we propose an IFM scheme based on the combination of Brillouin gain spectrum (BGS) and Brillouin loss spectrum (BLS), which is RF-power-independent with high measurement efficiency. The combination of BGS and BLS to construct the amplitude comparison function (ACF) can reduce the influence of RF signal power fluctuation within 21.27 dB by single-shot measuring. When an appropriate frequency interval with frequency domain monotonous power of microwave comb signal is modulated on the pump lightwave, the IFM accuracy of the unknown signal reaches about 1 MHz. After the initial calibration of the system, it can recognize the time-frequency variation of single tone signal, linear frequency modulated signal (LFM), nonlinear frequency modulated signal (NLFM), and Costas signal. This scheme will help to promote the application of the IFM in the field of spectrum reconnaissance and reception.**

***Index Terms*—Instantaneous frequency measurement, Brillouin gain and loss spectrum, power-independent, Costas signal.**

I. Introduction

THE instantaneous frequency measurement (IFM) of microwave signal is of vital importance in the scenery where requires continuous interception or identification of unknown signals [1], [2], such as communications, electronic warfare, cognitive radio systems, etc. The traditional electrical frequency measurement capability is restricted by the electronic component's bandwidth (<18 GHz) and vulnerable to electromagnetic interference. In contrast, the photonics-assisted IFM technology with its broad bandwidth, low cost [3], [4], and immunity against electromagnetic interference [5] has attracted great attention and development.

In the photonics-assisted IFM system, a series of schemes are realized by implementing photonics technology. Ref. [6] proposed an IFM scheme based on incoherent delay lines by using the incoherent characteristic of optical signals after two arms of the interferometers. Different fading responses were combined to create amplitude comparison function (ACF) for frequency measurement [7]–[10]. Although these schemes are power independent due to the power being removed by normalization of the reference arm in theory, the impacts of non-ideal responses of optical modulators such as their frequency chirp and finite extinction ratio (ER) could cause the ACF drift with the RF power [11]. Another kind of approaches were presented to measure RF frequency by using the frequency to time mapping technique [12]. The frequencies of unknown RF signals are mapped to several discrete time events. The time delays among these events are then measured to determine the unknown RF frequencies. By distinguishing different central wavelengths [14], [15] or directly introducing silicon photonic scanning devices [16], the above approach was further extended to measure multi-tune signals. On the basis of ensuring high frequency accuracy and large measurement range, the Ref. [17], [18] use the Brillouin opto-electronic oscillator to reduce the power of the signal to be measured to −67 dBm. However, subject to the rate of sweep signal, the measurement with high real-time requirements is not good, nor they could only measure the existence of frequency rather than the frequency varying with time. The combination of the above two types of methods' advantage proposed a new scheme based on scanning photonic filters [19]. Its principle is to construct ACF with different responses of optical filters, in which the photonic filters can be replaced by different photonics devices, including the Mach-Zehnder interferometer (MZI) [20], the polarization interferometer [21], Bragg gratings [22], [23], on-chip photonic filter [24].

This scheme mainly focused on improving the frequency measurement range and accuracy of single or multi-tone signals. For instance, Ref. [25] demonstrated the ability of measuring multi-tone signals with a wide range of 38 GHz and a high

Manuscript received 1 May 2022; revised 20 June 2022; accepted 23 June 2022. Date of publication 28 June 2022; date of current version 12 July 2022. This work was supported in part by the National Key Research and Development Program of China under Program 2019YFB2203700 and in part by the National Natural Science Foundation of China under Grant 61822508. *(Corresponding author: Wei-Wen Zou.)*

Xin Wang, Yong-Lan Yang, Yu-Qiu Xu, and Wei-Wen Zou are with the State Key Laboratory of Advanced Optical Communication Systems and Networks, Intelligent Microwave Lightwave Integration Innovation Center, Department of Electronic Engineering, Shanghai Jiao Tong University, Shanghai 200240, China (e-mail: wyxynsn@sjtu.edu.cn; yylsophia@sjtu.edu.cn; amayaq@sjtu.edu.cn; wzou@sjtu.edu.cn).

Yue Cao is with the Institute of Applied Optics, Xi'an 710065, China (e-mail: sherryyifan@126.com).

Digital Object Identifier 10.1109/JPHOT.2022.3186670

resolution of 1 MHz. Ref. [26] and [27] also achieved 20 GHz bandwidth within about 8 MHz accuracy measurement by using the Stimulated Brillouin scattering (SBS) effect. Similarly, Ref. [28] also make full use of narrowband filtering effect of SBS, and the accuracy of frequency measurement reaches about 1 MHz. But they all didn't exhibit very well for time-frequency variation signal.

To better characterize the time-frequency variation of a signal, we proposed a Brillouin IFM scheme based on SBS in optical fiber and carried out a proof-of-concept experiment successfully [25]. The SBS occurs in the fiber when satisfying the phase matching condition between lightwave and acoustic waves. For a typical two-terminal input system, the amplification process of the probe lightwave is equivalent to experience a Lorentz-profiled narrow-band filtering response produced by the pump light, which is the Brillouin gain spectrum (BGS). By the means of periodically changing the pump lightwave central wavelength, this scheme could achieve the information of frequency variation with time. We further optimized the SBS method via constructing an ACF through a microwave power ratio between two designed frequency responses to realize fast measurement [34]. Moreover, we improved the accuracy by applying a convolutional neural network [35]. But the measurement progress still needed to measure at least two times, which reduced the measurement efficiency and would bring practical application difficulties. In addition, this method could not measure multiple frequency components at the same time, because the gains of multiple frequency components will add up together. The detection after PD is the total gain, and there is no way to decouple it at present.

In this work, we propose a novel Brillouin IFM scheme by the combination of Brillouin gain spectrum (BGS) and Brillouin loss spectrum (BLS). Compared with Refs. [36], there is no need to measure the signal two times to generate an ACF. More importantly, due to the characteristics that the BGS and BLS occurred simultaneously, we successfully eliminate the influence of the unknown signal power fluctuations in the range of 21.27 dB and measure the time-frequency information of different frequency modulation signals. When an appropriate frequency interval with frequency domain monotonous power of a microwave comb signal is modulated on the pump lightwave, it can achieve high frequency measurement accuracy with root-mean-square error (RMSe) less than 1 MHz of 100 MHz bandwidth at X band (10.53–10.63 GHz). Furthermore, a series of signals involving linear frequency (LFM) signal, nonlinear frequency (NLFM) signal, and Costas signal with 2 GHz bandwidth (20 GHz–22 GHz) are measured and recognized. This scheme solves the contradiction between power fluctuation and frequency measurement efficiency of an unknown signal in Brillouin IFM method.

II. Principle and Experiment Setup

The main principle of this scheme is the Brillouin gain and loss effects. The SBS is an energy transfer between two lightwaves that satisfy the phase matching condition, that is, the frequency difference equals to the Brillouin frequency shift

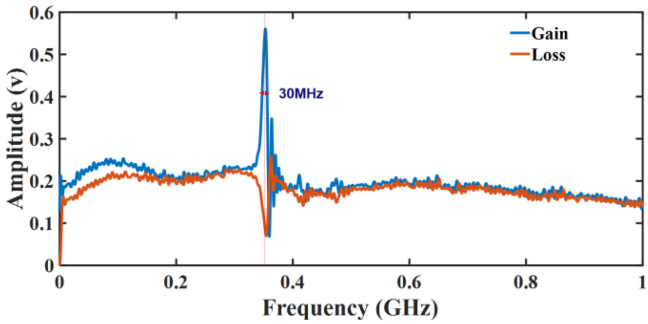

Fig. 1. Brillouin gain and loss spectra.

(BFS) of the Brillouin medium. There are three lightwaves f_{p0} ,f_{p1} and $f_{p2}$with frequencies $f_{p1} < f_{p0} < f_{p2}$, where f_{p0} and f_{p1} propagate opposite to each other f_{p0} and f_{p2} propagate opposite to each other. If their frequency intervals are both equal to the BFS, the energy will be transferred from the lightwave with the higher frequency to the lightwave with the lower frequency. The lightwave with the frequency f_{p0} causes the amplification of the frequency f_{p1} and the attenuation of the frequency f_{p2}. As a result, the pump lightwave with a frequency f_{p0} introduces a gain spectrum (BGS) and a loss spectrum (BLS) at the relatively low and high frequencies of two separate lightwaves, respectively. The intrinsic spectral line width of the gain spectrum or loss spectrum is about 30 MHz, which is mainly determined by the optical fiber structure and pump power [36]. Fig. 1 shows the Brillouin gain and loss spectra at low and high frequencies of the same pump light.

Further, if the pump lightwave is extended to the form of optical frequency comb (OFC) whose interval is less than the BGS line width, each comb tooth will act as a single pump lightwave after being modulated to a single wavelength continuous lightwave [37]. The BGSs and BLSs generated by multiple pumps could be superimposed to become broaden. Coupled with flexible design of the power of each tooth of the frequency comb, the desired form of gain and loss spectrum profiles can be achieved. It should be noted that it is hard to generate an OFC with single tooth power tunable by optical method. Here, we use microwave frequency comb to modulate a continuous-wave lightwave.

Fig. 2 demonstrates the principle of the initial calibration ACF and subsequent process of measuring the unknown frequency. In order to obtain two frequency response curves with opposite trends, we set the powers of the comb teeth to a linear change, as shown near the pump lightwave fc on the frequency axis in Fig. 2. A Brillouin gain region and a loss region are generated at the BFS locations away from the upper and lower sidebands of the pump lightwave. It is realized by a carrier suppressed double band modulation (CSDB). The measurement bandwidth is determined by the spectrum range covering the microwave frequency comb. An LFM signal with known frequency and power parameters is used for calibration and modulated on the probe lightwave by intensity modulation. It is shown as two rectangles in Fig. 2. The up and down sidebands of the probe lightwave would be amplified and attenuated at every moment

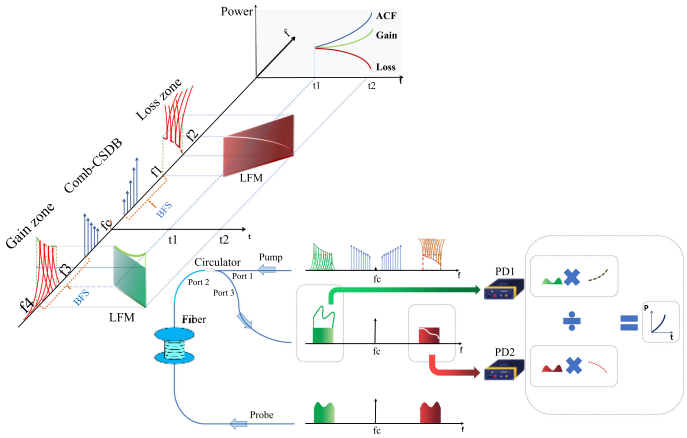

Fig. 2. Schematic of power-independent IFM based on combination of the BGS and BLS.

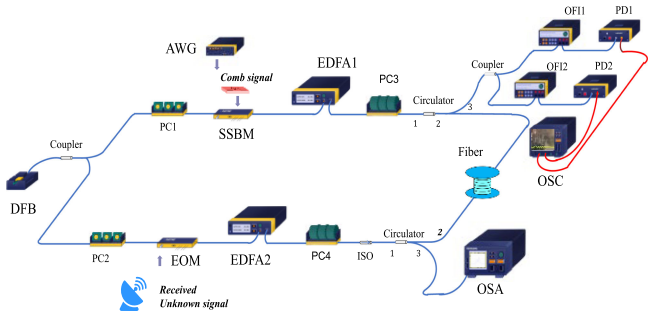

Fig. 3. Experimental setup of the power independent IFM system, DFB: distributed-feedback laser, PC: polarization controller, AWG: arbitrary waveform generator, SSBM: single sideband modulator, EOM: electro-optic modulator, EDFA: erbium-doped fiber amplifier, ISO: isolator, PD: photodetector, OFI: optical filter, OSC: oscilloscope, OSA: optical spectrum analyzer.

by the broadened BGS and BLS, respectively. Two optical filters are used to filter out the signals' up and down sidebands whose envelopes are detected by two low-bandwidth PDs later. The envelope monotonicity is determined by the power monotonicity of microwave frequency comb spectrum and a mapping relationship is established between the power and frequency through the duration of the LFM signal.

The effect of LFM power fluctuation could be easily eliminated by normalization between gain and loss envelops, which also increases the steep degree of the ACF curve. The ACF curve obtained can be expressed as:

$$ACF = \frac{1 + G(f)}{1 - L(f)} \tag{1}$$

where $G(f)$ and $L(f)$ represent the convolution results of the microwave frequency comb envelope with the intrinsic BGS and BLS, respectively. The pump lightwave modulated by the microwave frequency comb can improve the accuracy because it is more stable in generating SBS effect than the NFLM signal [33] where the Brillouin gain is determined by the speed of frequency sweeping. Smaller comb interval means more intense at the Brillouin gain peak superposition place which can bring smoother ACF.

The experimental setup of the IFM system is depicted in Fig. 3. The optical lightwave is provided by a tunable laser source (CW, TLG-200, Alnair Labs) with a power of 15 dBm. A 50:50 coupler divides the 1550 nm optical lightwave into the upper branch and the lower branch, whose polarization states are controlled by polarization controllers (PCs) 1–4, respectively.

The lightwave in the upper branch enters the single sideband modulator (IXBLUE MXIQER-LN-30-PD) is modulated by the RF frequency comb signal in the form of carrier suppressed double sideband modulation. The input RF frequency comb signal is generated by the AWG (Keysight M8195A). The frequency comb signal ranges from 10.53 to 12.53 GHz, and the BFS of the optical fiber is 9.47 GHz. Hence, the frequency range of the signal to be measured is 20–22 GHz. The power variation range of the frequency comb is controlled at 30 dB. The modulated lightwave is amplified to 20 dBm by an erbium-doped fiber amplifier (EDFA1), so that the SBS effect is more sufficient. After the polarization control of PC3, the amplified pump light is coupled into a dispersion-compensation fiber (DCF) with a length of 200 m through the first port of circulator 1. The fiber insertion loss is 4 dB and the Brillouin gain coefficient is 6.9 m/W [38].

The lightwave in the lower branch is modulated by an electro-optic intensity modulator (EOM) (EO Space, AX-0MVS-40-PFA-PFA). An LFM signal used for the initial calibration has a duration of 1 μs and varies in frequency from 20 to 22 GHz. When the calibration is finished, the RF input port of the EOM is used to receive the unknown signal. The EDFA2 is used to amplify the modulated lightwave signal to keep its output at 10 dBm and the isolator (ISO) could isolate the reflected pump lightwave. The amplified lightwave is then put into the DCF through the port 2 of the circulator 2, in which the SBS effect occurs. The lightwave after SBS output through the port 3 of the circulator 1, which is divided by another 50:50 coupler. The two signals pass through two optical band pass filters (BVF-300CL-SM-FA), respectively. Finally, the gain and loss envelopes are detected by two PDs (FS-PD-B-2030, Fsphotonics) with a 500 MHz bandwidth and recorded by an oscilloscope (Infinium UXR0134A, Keysight).

III. Experimental Results

A. Pump Signal and IFM Accuracy

First, we study the effect of the microwave frequency comb form. Figs 4(a) and (b) present the microwave frequency comb signal in time domain and frequency domain, the waveform is periodic due to the superposition of multiple sine waves with a certain phase relationship. In the frequency domain, the amplitude of the frequency comb shows a monotonically rising state, which benefits from the power setup of each comb tooth. The profile of the spectrum determines the shape of the ACF. It should be noted that the comb power in Fig. 4(b) is not very smooth, which is due to the low quality of the comb generated from AWG in such a high frequency band. This will make the ACF not smooth as plotted in Fig. 4(c) and might bring a worse measurement error. The ACF is relatively flat because for a probe

TABLE I
COMPARISON OF ADVANCED FREQUENCY MEASUREMENT

Ref.	institution	Range (GHz)	Accuracy（MHz）	Time-Frequency Information	Power Independent
[25]	University of Sydney	9-38	≤1	No	Yes
[16]	Huazhong University	1-30	237.3	No	Yes
[21]	Beijing Jiaotong University	0-25	±200	No	Yes
[28]	East China Normal University	6-18	±1	No	Yes
[29]	East China Normal University	0.3-7.6	≤1	No	No
This work	Shanghai Jiao Tong University	10.53-10.63	≤1	Yes	Yes
		20-22	30		

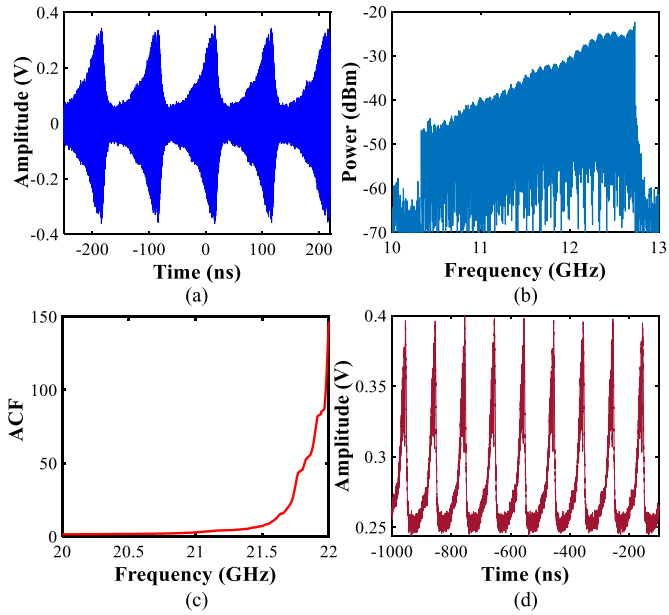

Fig. 4. Microwave frequency comb signal in (a) time domain and (b) frequency domain. (c) ACF produced by comb's modulated pump lightwave. (d) Comb modulated pump lightwave detected by PD.

signal, each tooth of the pump frequency comb corresponds to a pump lightwave, and each tooth produces a Brillouin gain spectrum of Lorentz shape. When the multiple Brillouin gain spectra generated by frequency comb are superimposed, the whole gain (or loss) is similar to a larger Lorentz-shaped gain spectrum, and the ACF is half of the larger gain spectrum, resulting in this shape showed a relatively flat front and steep back end. Fig. 4(d) is the profile of the frequency comb in the optical domain obtained after PD, which is actually closer to the shape of an ACF.

In order to verify the relationship between the comb pump and the IFM accuracy, we reduce the bandwidth of frequency measurement and the comb tooth interval is 5 MHz. Fig. 5 depicts the measurement of Costas signal at 10.53–10.63 GHz when the pump signal is 1.06-1.16 GHz, respectively. The blue solid curve in Fig. 5(a) denotes the envelope of the LFM (1 μs, 10.53–10.63 GHz) signal gain curve obtained after the broadened BGS amplifying one of the probe lightwave sidebands through the optical filter and PD. Accordingly, the black dot line represents the envelope of loss. Before the SBS occurs, the envelopes of two probe lightwave sidebands should be equal to ensure the consistency of initial state by adjusting the optical attenuator. Fig. 5(b) shows the envelope ratio of gain curve to loss curve, namely ACF. Obviously, it can be seen from Figs. 5(c) and (d) that the measured frequency hopping signal encoded by Costas is in a good agreement with the theoretical value. The maximum error is within ±2 MHz, and the RMSe is 1 MHz. Smoother comb produces smoother ACF curves. In fact, the best ACF curve should only be as linear as possible, which can minimize the measurement error. To update, none of the

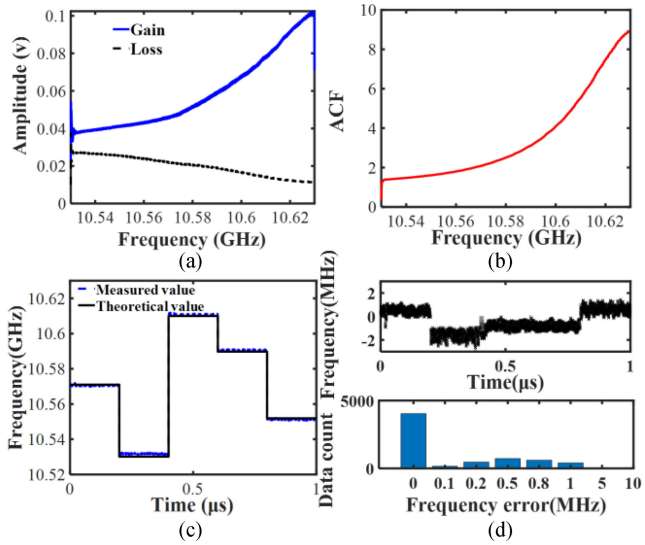

Fig. 5. IFM results with 100-MHz bandwidth and 1-MHz precision. (a) Gain and loss envelope of LFM signal after SBS. (b) ACF of gain divide loss. (c) Measured Costas signal and theoretical Costas signal. (d) Error statistics.

conventional ACF based schemes produced a truly linear ACF curve even in theory. Nevertheless, our comb's scheme has the potential to produce a more linear ACF curve by designing every broach's power, which will be studied in the further research.

B. Power Independent IFM of the Unknown Signal

As mentioned above, our scheme could eliminate the influence of the unknown signal power fluctuation due to the gain and loss envelopes being reflected in the same time. To verify this ability, we design an amplitude hopping, frequency continuous linear change signal. Subject to the limitation of AWG output, the maximum peak-to-peak voltage (V_{pp}) is about 1 V, the minimum V_{pp} is about 75 mV. The power variation range in theory is $20 \cdot log(1000/75) = 22.5$ dB. Fig. 6(a) demonstrates the real output power range about 21.27 dB of the designed signal, which is a little different from the theory range (22.5 dB). Fig. 6(b) shows the variation of its power, time, and frequency by short-time Fourier transform (STFT). Fig. 6(c) presents the statistics of measurement frequency and its error. It can be seen that even if the signal with the power hopping change, it can also recover the information of time-frequency variation. The RMSe is 30 MHz. Around 20 GHz, the error is relatively large. We consider that this is mainly due to the low power of the frequency comb here, resulting in a small gain and loss effect. However, in the higher frequency range, the power hopping does not affect the measurement of frequency, so there should be a minimum detectable power, above the minimum power of the unknown signal is to satisfy power - frequency characteristics. This minimum detectable power is determined by the pump signal modulated by the local frequency comb.

In addition, it should be noted that the modulator and optical filter frequency response could also impact the envelopes of the probe lightwave sidebands. To overcome this impact, we should carry out a certain calibration process according to the frequency

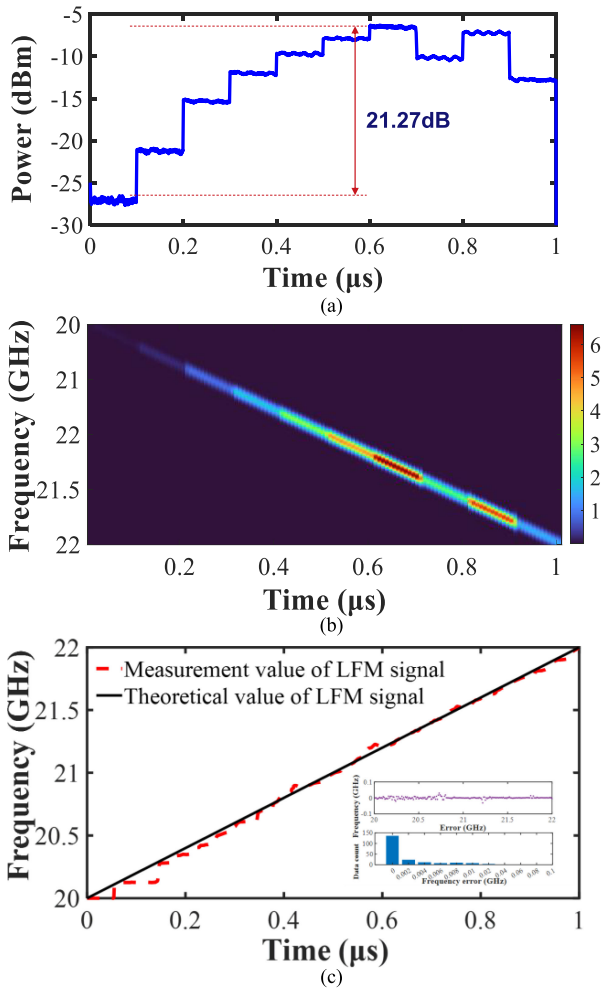

Fig. 6. (a) Amplitude hopping, frequency continuous linear change signal. (b) Short-time Fourier transform (STFT) of the designed signal. (c) Measurement of the designed signal.

response of the modulator and optical filter by introducing the optical attenuator.

C. Multiple Frequency Modulated Signal Types

We tested 200 different frequency continuous sinewave signals in the middle range of 20 GHz–22 GHz by stepping at 10 MHz. Figure 7(a) reveals the relationship between the input signal and the output signal frequency. Subsequently, the scheme not only measures the existence of frequency, but also recognizes the variation of frequency with time. We further measure several other frequency modulation signals. Figs 7(b) and (c) correspond to two kinds of nonlinear frequency modulation signals and Fig. 7(d) to a Costas signal, respectively. The RMSEs are at the level of 30 MHz. The ACF used for measurement here is shown in Fig. 4(d). The smoothness of the ACF is not good as shown in Fig. 5(b). The error is a little worse than that of a smooth one. From Fig. 7, we can recognize the frequency modulation type of each signal. This scheme further improves the frequency measurement and recognition ability of the IFM system base SBS.

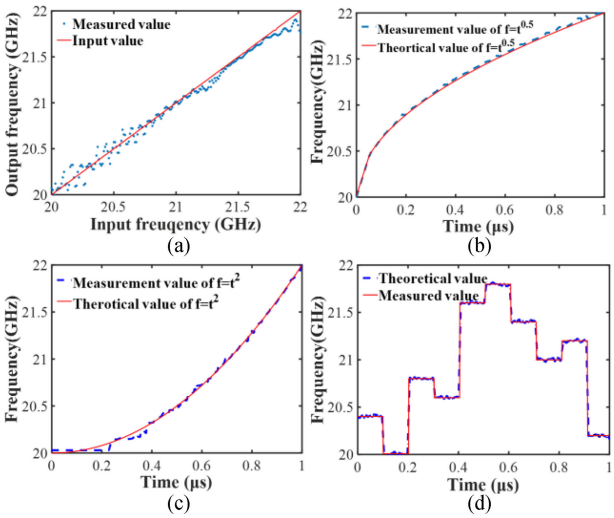

Fig. 7. Measurement of signals modulated at different frequencies. (a) Single frequency continuous optical signal. (b) NLFM signal of $f = t^{0.5}$. (c) NLFM signal of $f = t^2$. (d) Costas signal.

IV. Discussion

We compare the important performance of this IFM system to those of other state-of-the art IFM techniques in Table I. The power-independent IFM system based on combination of BGS and BLS mainly have the following advantages:

1. The ability of measuring unknown signals whose frequency varies continuously with time. Although Ref. [25] has reached a frequency step time of about tens of nano seconds, it still belongs to the category of frequency scanning change and is not the time-frequency measure of instantaneous signals in the real sense. 2. Simplifying the Brillouin time-frequency information measurement process. The scheme based on power-frequency mapping in [33]–[35] need to measure two times Brillouin gain to get the ACF, which means when measuring the unknown signal measurement, also need to measure two times gain of one signal. This increases the complexity of operation and reduces the significance of frequency measurement system in intercepting unknown signal. 3. The frequency comb breaks out the limitation error of Brillouin method. In reference [21], [28]–[29], the error of frequency measurement is mainly determined by the line width of BGS. In order to reduce the error, an additional method of reducing the BGS line width has to be introduced. However, the scheme in this work achieves monotonic gain and reduces system error at the same time by controlling the amplitude of frequency comb. It should also be noted that comb's form of amplitude variation is not limited to linear variation. True linearization of the ACF curve can also be achieved through special design, and this part of improvement is under further study.

V. Conclusion

We have demonstrated the proposed IFM system based on the combination of BGS and BLS have the power-independent characteristics with efficiency measurement. The experiment verifies the measurement of the LFM signal within the power fluctuation range of 21.27 dB, achieving the accuracy of 1 MHz in the X band with the bandwidth of 100 MHz and 30 MHz in the K band with the bandwidth of 2 GHz bandwidth. We have further presented the measurement of the single frequency continuous optical signal, NLFM signal, and the frequency hopping signal of time series encoding. Our method provides the potential for IFM in the field of spectrum reception and recognition in practical applications with strong power fluctuation.

References

[1] R. G. Wiley *et al.*, *Electronic Intelligence: The Analysis of Radar Signals*. Boston, MA, USA: Artech House, 1993, ch.1, pp. 13–14.
[2] A. E. Spezio, "Electronic warfare systems," *IEEE Trans. Microw. Theory Techn.*, vol. 50, no. 3, pp. 633–644, Mar. 2002.
[3] J. Capmany, J. Mora, I. Gasulla, J. Sancho, J. Lloret, and S. Sales, "Microwave photonic signal processing," *J. Lightw. Technol.*, vol. 31, no. 4, pp. 571–586, Feb. 2013.
[4] S. Pan and J. Yao, "Photonics-based broadband microwave measurement," *J. Lightw. Technol.*, vol. 35, no. 16, pp. 3498–3513, Aug. 2017.
[5] J. Tsui, *Microwave Receivers with Electronic Warfare Applications*. Raleigh, NC, USA: SciTech, 2005.
[6] L. A. Bui and A. Mitchell, "Instantaneous frequency measurement using optical coherence and DC photodetection," in *Proc. IEEE Int. Topical Meeting Microw. Photon.*, 2010, pp. 358–360.
[7] L. A. Bui, N. Sarkhosh, and A. Mitchell, "Photonic instantaneous frequency measurement: Parallel simultaneous implementations in a single highly nonlinear fiber," *IEEE Photon. J.*, vol. 3, no. 5, pp. 915–925, Oct. 2011.
[8] L. A. Bui and A. Mitchell, "Parallel all-optical instantaneous frequency measurement system using channel labeling," *IEEE Photon. Technol. Lett.*, vol. 24, no. 13, pp. 1118–1120, Jul. 2012.
[9] L. A. Bui and A. Mitchell, "Amplitude independent instantaneous frequency measurement using all optical technique," *Opt. Exp.*, vol. 21, no. 24, pp. 29601–29611, Dec. 2013.
[10] M. Ganjali and S. E. Hossein, "Effects of frequency chirping and finite extinction ratio of optical modulators in microwave photonic IFM receivers," *Opt. Commun.*, vol. 452, pp. 380–386, 2019.
[11] C. Yang, L. Wang, and J. Liu, "Photonic-assisted instantaneous frequency measurement system based on a scalable structure," *IEEE Photon. J.*, vol. 11, no. 3, Jun. 2019, Art. no. 5501411.
[12] T. A. Nguyen, E. H. W. Chan, and R. A. Minasian, "Instantaneous high-resolution multiple-frequency measurement system based on frequency-to-time mapping technique," *Opt. Lett.*, vol. 39, no. 8, pp. 2419–2422, 2014.
[13] L. V. T. Nguyen, "Microwave photonic technique for frequency measurement of simultaneous signals," *IEEE Photon. Technol. Lett.*, vol. 21, no. 10, pp. 642–644, May 2009.
[14] T. A. Nguyen, E. H. W. Chan, and R. A. Minasian, "Photonic multiple frequency measurement using a frequency shifting recirculating delay line structure," *J. Lightw. Technol.*, vol. 32, no. 20, pp. 3831–3838, Oct. 2014.
[15] S. Wang, G. Wu, Y. Sun, and J. Chen, "Photonic compressive receiver for multiple microwave frequency measurement," *Opt. Exp.*, vol. 27, no. 18, pp. 25364–25374, 2019.
[16] W. Xu *et al.*, "Wideband adaptive microwave frequency identification using an integrated silicon photonic scanning filter," *Photon. Res.*, vol. 7, no. 2, pp. 172–181, 2019.
[17] Z. Zhu *et al.*, "Highly sensitive, broadband microwave frequency identification using a chip-based Brillouin optoelectronic oscillator," *Opt. Exp.*, vol. 27, no. 9, pp. 12855–12868, 2019.
[18] G. Wang *et al.*, "Detection of wideband low-power RF signals using a stimulated Brillouin scattering-based optoelectronic oscillator," *Opt. Commun.*, vol. 439, pp. 133–136, 2019.
[19] J. S. Fandino and P. Munoz, "Photonics-based microwave frequency measurement using a double-sideband suppressed-carrier modulation and an InP integrated ring-assisted Mach–Zehnder interferometer filter," *Opt. Lett.*, vol. 38, no. 21, pp. 4316–4319, 2013.
[20] J. S. Fandiño and P. Muñoz, "Analysis of system imperfections in a photonics-assisted instantaneous frequency measurement receiver based on a dual-sideband suppressed-carrier modulation," *J. Lightw. Technol.*, vol. 33, no. 2, pp. 293–303, Jan. 2015.
[21] J. Li, L. Pei, T. Ning, J. Zheng, Y. Li, and R. He, "Measurement of instantaneous microwave frequency by optical power monitoring based on polarization interference," *J. Lightw. Technol.*, vol. 38, no. 8, pp. 2285–2291, 2020.

[22] Z. Li *et al.*, "Photonic instantaneous measurement of microwave frequency using fiber Bragg grating," *Opt. Commun.*, vol. 283, no. 3, pp. 396–399, 2010.
[23] Z. Li, C. Wang, M. Li, H. Chi, X. Zhang, and J. Yao, "Instantaneous microwave frequency measurement using a special fiber Bragg grating," *IEEE Microw. Wireless Compon. Lett.*, vol. 21, no. 1, pp. 52–54, Jan. 2011.
[24] B. Zhu, W. Zhang, S. Pan, and J. Yao, "High-sensitivity instantaneous microwave frequency measurement based on a silicon photonic integrated Fano resonator," *J. Lightw. Technol.*, vol. 37, no. 11, pp. 2527–2533, Jun. 2019.
[25] H. Jiang *et al.*, "Wide-range, high-precision multiple microwave frequency measurement using a chip-based photonic Brillouin filter," *Optica*, vol. 3, pp. 30–34, 2016.
[26] X. Long, W. Zou, and J. Chen, "Broadband instantaneous frequency measurement based on stimulated Brillouin scattering," *Opt. Exp.*, vol. 25, no. 3, pp. 2206–2214, 2017.
[27] D. Wang *et al.*, "Photonic microwave frequency measurement with improved resolution based on bandwidth-reduced stimulated Brillouin scattering," *Opt. Fiber Technol.*, vol. 68, 2022, Art. no. 102803.
[28] J. Liu, T. Shi, and Y. Chen, "High-accuracy multiple microwave frequency measurement with two-step accuracy improvement based on stimulated Brillouin scattering and frequency-to-time mapping," *J. Lightw. Technol.*, vol. 39, no. 7, pp. 2023–2032, Apr. 2021.
[29] T. Shi and Y. Chen, "Multiple radio frequency measurements with an improved frequency resolution based on stimulated Brillouin scattering with a reduced gain bandwidth," *Opt. Lett.*, vol. 46, no. 14, pp. 3460–3463, 2021.
[30] D. Wang *et al.*, "Photonic-assisted microwave frequency measurement with adjustable channel bandwidth based on spectrum-controlled Brillouin phase shift," *IEEE Photon. J.*, vol. 13, no. 6, Dec. 2021, Art. no. 5500205.
[31] W. Jiao, K. You, and J. Sun, "Multiple microwave frequency measurement with improved resolution based on stimulated Brillouin scattering and nonlinear fitting," *IEEE Photon. J.*, vol. 11, no. 1, Feb. 2019, Art. no. 5500912.
[32] D. Wang *et al.*, "Wide-range, high-accuracy multiple microwave frequency measurement by frequency-to-phase-slope mapping," *Opt. Laser Technol.*, vol. 123, 2020, Art. no. 105895.
[33] X. Long, W. Zou, and J. Chen, "Broadband instantaneous frequency measurement based on stimulated Brillouin scattering," *Opt. Exp.*, vol. 25, no. 3, pp. 2206–2214, 2017.
[34] W. Zou *et al.*, "Brillouin instantaneous frequency measurement with an arbitrary response for potential real-time implementation," *Opt. Lett.*, vol. 44, no. 8, pp. 2045–2048, 2019.
[35] X. Zou *et al.*, "Optimization of the Brillouin instantaneous frequency measurement using convolutional neural networks," *Opt. Lett.*, vol. 44, no. 23, pp. 5723–5726, 2019.
[36] W. Zou, Z. He, and K. Hotate, "Two-dimensional finite-element modal analysis of Brillouin gain spectra in optical fibers," *IEEE Photon. Technol. Lett.*, vol. 18, no. 23, pp. 2487–2489, Dec. 2006.
[37] T. Sakamoto *et al.*, "Low distortion slow light in flat Brillouin gain spectrum by using optical frequency comb," *Opt. Exp.*, vol. 16, no. 11, pp. 8026–8032, 2008.
[38] Y. Ji *et al.*, "Signal-to-noise ratio enhancement of stimulated Brillouin scattering based pulse compression of an ultrabroad microwave signal by use of a dispersion compensation fiber," *Opt. Lett.*, vol. 42, no. 15, pp. 2980–2983, 2017.